



Optimisation of microwave-assisted production of acid condensate from palm kernel shell and its biological activities

Seri Elyanie Zulkifli¹ · Mohd Amir Asyraf Mohd Hamzah¹ · Maizatulakmal Yahayu² · Astimar Abd. Aziz³ · Najihah Mohd. Hashim⁴ · Zainul Akmar Zakaria¹

Received: 11 April 2021 / Revised: 27 May 2021 / Accepted: 3 June 2021 / Published online: 15 June 2021
© The Author(s), under exclusive licence to Springer-Verlag GmbH Germany, part of Springer Nature 2021

Abstract

This study reports on the microwave-assisted heating optimisation of acid condensate (AC) from palm kernel shell (PKS), using the central composite design (CCD) approach focusing on its total phenolic content (TPC) as response and its antimicrobial activity. Thermogravimetric-derivative thermogravimetric (TG-DTG) analysis clearly depicted the devolatilisation of lignocellulosic content of PKS. The highest TPC in concentrated AC extract (CACE), $451.51 \pm 2.37 \mu\text{g GAE/mg}$ (R^2 0.9870), was obtained at microwave power of 580 W, nitrogen flow rate of 2.4 L/min and final temperature of 480 °C. Nitrogen flow rate had the highest effect on TPC with an F value of 63.65. Relative to ascorbic acid, CACE showed a higher Trolox equivalent antioxidant capacity (TEAC) but almost similar 2,2-diphenyl-1-picrylhydrazyl (DPPH) radical scavenging capabilities which can be attributed to the presence of 1,2-benzendiol, i.e. catechol (27.82%) and 1,3-dimethoxy-2-hydroxybenzene, i.e. syringol (22.76%). CACE also displayed good potential for antimicrobial application with high growth inhibition of *Escherichia coli*, *Pseudomonas aeruginosa*, *Staphylococcus aureus*, *Enterococcus faecalis*, *Aspergillus niger* and *Fusarium oxysporum*. In conclusion, PKS has a great potential to be used as raw material to produce AC (acid condensate) using microwave-assisted heating process.

Keywords Palm kernel shell · Acid condensate · Optimisation · Antioxidant · Antimicrobial

1 Introduction

As the second largest producer of palm oil in the world, Malaysia produced large amount of oil palm biomass such as palm kernel shell (PKS), oil palm fronds and mesocarp fibre [1]. Improper biomass waste management may lead to anaerobic degradation into greenhouse gases such as methane.

One of the approaches available to manage the abundance of oil palm biomass is through thermochemical conversion method such as microwave-assisted pyrolysis which is a method of heating the substances in the absence of oxygen that yielded biochar, bio-oil, biogas and acid condensate [2].

Acid condensate (AC), also known as wood vinegar, is an acidic reddish-brown aqueous liquid obtained from the condensation of gaseous parts generated during the pyrolysis process. AC has acidic pH of around 2.5–3.5 and consists several groups of valuable organic compounds such as organic acids, phenols, aldehydes, alcohols, ketones, pyran, furan derivatives and polyphenolic compounds [3]. In order to obtain AC with high yield of phenolic compounds and its derivatives, PKS has been the subject of interest due to its high amount of lignin content which correlates to the yield of phenolic compounds [4] that is responsible to the high antioxidant properties of AC [5].

For decades, uncontrolled growth of bacteria and fungi has been a major concern in agricultural, environment and human and animal health since its presence resulted in human, animal and plant diseases and low-yielding

✉ Zainul Akmar Zakaria
zainulakmar@utm.my

¹ School of Chemical and Energy Engineering, Faculty of Engineering, Universiti Teknologi Malaysia, 81310 Johor Bahru, Johor, Malaysia

² Institute of Bioproduct Development, Universiti Teknologi Malaysia, 81310 Johor Bahru, Johor, Malaysia

³ Engineering and Processing Research Division, Malaysian Palm Oil Board, No.6, Persiaran Institusi, Bandar Baru Bangi, 43000 Kajang, Selangor, Malaysia

⁴ Department of Pharmaceutical Chemistry, Faculty of Pharmacy, University of Malaya, 50603 Kuala Lumpur, Malaysia

production quality [6]. AC offers a promising alternative for antibiotic and chemicals for treatment of human and plant against microbiological infections/attacks as AC exhibits antibacterial [7], termiticidal [8], antifungal [9], anti-inflammatory [10], herbicide [11] and antibiotic in poultry [12]. In addition, AC is considered low cytotoxic at 100-fold dilution [13] and does not pose severe hazard to the environment [14].

In view of this, this study highlights on optimisation of AC using response surface methodology (RSM) based on the central composite design (CCD) approach as it offers a better alternative to the full factorial three-level design since it demands a smaller number of experiments while providing comparable results [15] and better prediction than other optimisation designs [16]. This study also focuses on the elaboration of the potential inhibitory effect of AC compounds obtained from microwave-assisted heating of PKS towards bacteria and fungi species. This is the first report on the optimisation of TPC in AC from PKS (termed as AC-PKS) using RSM.

2 Materials and methods

2.1 Sample preparation and characterisation of PKS

The PKS samples were obtained from one local palm oil mill in Johor, Malaysia. The sample was washed using tap water, sun-dried for 3 days and grounded (Df-25 automatic herb grinder, DA DE brand) to 1–3 mm using facilities available in one commercial laboratory located in Kota Tinggi, Johor. The American Society for Testing and Materials (ASTM) were used to characterise the moisture content (ASTM E 1756), ash (ASTM E1755-01) and volatile matter (ASTM D3714). The standard laboratory analytical procedure (LAP) was used to determine the lignin (LAP-003, 004) and cellulose (LAP-002) contents. The thermogravimetric analysis of PKS was carried out using the Pyris-6 thermogravimetric analyser (Perkin Elmer) as described by Mensah et al. [17]. PKS sample was grounded further and sieved to mesh size between 105 and 120 μm prior to heating at 30–600 °C using nitrogen gas followed by at 600–800 °C by using oxygen gas, both at a fixed heating rate of 25 °C/min.

2.2 Microwave-assisted pyrolysis of PKS

The experimental rig was set up according to Abas et al. [18] with slight modification as follows: the microwave-assisted pyrolysis of PKS was carried out using microwave oven (MW71B, Samsung) with 800 W maximum output power and 2.45 GHz frequency at the Combustion Lab, School of Mechanical Engineering, Universiti Teknologi. This pyrolysis system setup consists of fabricated

microwave, temperature controller, quartz glass reactor, N_2 supply, thermocouple type R, glass tube connector, condenser, water chiller (Alpha R8-Lauda, Germany), lab jack, flat bottom flask and PicoLog data logger. The cylindrical quartz glass reactor with top and bottom flange was designed in the size of 100 mm (ID), 150 mm (OD) and 205 mm in height. The 100-mm ID flange lid glasses, Favorit brand, were used to cover both top and bottom of the quartz glass reactor. One hundred g of PKS was mixed with commercial granulated activated charcoal (n-2, 3–5 mm, MW-12.01 g/mol HmbG). Nitrogen gas was then supplied from the top of the reactor at 10 L per minute (L/min) for 15 min prior to the start of pyrolysis to ensure inert environment inside the quartz glass reactor. The water chiller was maintained at 6–7 °C, and the reaction time was kept constant at 60 min. The thermocouple type R that was connected to the PicoLog data logger system was inserted directly on top of the sample. A series of condenser units were installed to condense vapours into AC liquid. The liquid and solid products were collected and weighed after pyrolysis process to determine the percentage yield of solid, liquid and gaseous products obtained.

2.3 Optimisation of AC production

Response surface methodology, RSM (via Design-Expert software version 7) was used to carry out optimised production of AC by microwave-assisted heating. Three different factors (final microwave temperature, microwave power, nitrogen flow rate) with TPC as the response were studied using central composite design (CCD) approach. The details of the experimental level of three factors with coded value (1 for high level and –1 for low level) followed by the 17 standard runs including replicated of 3 central points (run), 1 factorial point and 1 axial points were tabulated as shown in Table 1. AC obtained was collected and filtered followed by extraction using ethyl acetate (EA) AR grade at a 1:1 ratio [19]. The mixtures were homogeneously shaken for 3 min and let to stand for 30 min to allow phase separation. The top organic layer (representing EA) was collected, while the bottom aqueous layer was extracted for a second time using fresh EA. The combined AC extracts were then concentrated using rotary evaporator (120 mBar, 80 °C, Heidolph, Germany) until small volume was obtained and termed as concentrated AC extract (CACE). The CACE was then placed in a desiccator for 3–5 days to remove excess water. AC was extracted using EA to obtain an optimum total phenolic content, as EA is a medium polar solvent with polarity index of 4.4. The effectiveness of natural bioactive effects depends more on the type of solvents used for the extraction rather than the wood source [20].

Table 1 Optimisation of TPC in CACE using RSM

Std	Run	Factor A: final temperature (°C)		Factor B: micro-wave power (watts)		Factor C: nitrogen flow rate (L/min)		Experimental output: TPC (µg GAE/mg sample)
		Actual	Coded	Actual	Coded	Actual	Coded	
1	2	300	-1.0	350	-1.0	1.0	-1.0	254.8
2	6	600	1.0	350	-1.0	1.0	-1.0	190.12
3	4	300	-1.0	800	1.0	1.0	-1.0	273.46
4	14	600	1.0	800	1.0	1.0	-1.0	301.2
5	5	300	-1.0	350	-1.0	5.0	1.0	317.85
6	11	600	1.0	350	-1.0	5.0	1.0	267.21
7	13	300	-1.0	800	1.0	5.0	1.0	330.05
8	9	600	1.0	800	1.0	5.0	1.0	371.85
9	1	198	-1.7	575	0.0	3.0	0.0	362.52
10	17	702	1.7	575	0.0	3.0	0.0	344.84
11	3	450	0.0	200	-1.7	3.0	0.0	209.16
12	7	450	0.0	800	1.7	3.0	0.0	296.15
13	10	450	0.0	575	0.0	1.0	-1.7	255.40
14	15	450	0.0	575	0.0	6.4	1.7	342.00
15	12	450	0.0	575	0.0	3.0	0.0	480.01
16	16	450	0.0	575	0.0	3.0	0.0	455.15
17	8	450	0.0	575	0.0	3.0	0.0	434.39

2.4 TPC and chemical characterisation of CACE

The TPC in CACE was determined as follows [10]: a mixture of 1 mL of the CACE extract and 1 mL of 50% v/v of Folin Ciocalteu reagent was added with 1 mL of 10% w/v sodium carbonate and left for 2 h at ambient temperature. The optical density of the mixture was measured at 765 nm (UV-1800, Shimadzu, Japan). Gallic acid was used to plot the calibration curve. The TPC determined was expressed as µg gallic acid equivalent/mg of dried sample (µg GAE/ mg). The 2,2-diphenyl-1-picrylhydrazyl (DPPH) assay was performed as follows: a mixture of 1 mL of CACE extract and 2 mL of methanolic DPPH reagent was vortexed and allowed to stand for 30 min at room temperature. The optical density was measured at 517 nm using methanol as blank. Trolox equivalent antioxidant capacity (TEAC) was carried out using method proposed by Re et al. [21] where a mixture of 0.3 mL sample (20 µg/mL) and 2.7 mL of the ABTS^{•+} solution was incubated at 37 °C for 7 min. ABTS^{•+} solution was prepared by mixing 7 mM of ABTS solution with 2.45 mM potassium persulphate solution at a 1:1 ratio. The optical density of the mixture was measured at 734 nm. Trolox was used as standard curve. The reducing antioxidant activity of the CACE is expressed as Trolox equivalent/g dried sample (µg TE/mg sample).

2.5 Gas chromatography–mass spectrometry (GC–MS)

The CACE was analysed for chemical compositions using gas chromatography–mass spectrometry (GC–MS, QP500,

Shimadzu, Japan) using the method suggested by Abas et al. [18]; CACE (100 µl) was dissolved in 2 ml of 95% methanol HPLC grade and filtered using 0.2-µm membrane syringe filter. One µl of filtered sample was injected with a split rate of 20:1 into the capillary column (BXP-5) with a diameter of 29.4 m × 0.25 mm. The injector pressure and split flow rate were 10.97 psi and 23.8 mL/min, respectively. The helium gas was used as a carrier gas, and the temperature of injector was at 300 °C. The final temperature around 325 °C was held for 10 min, and each sample was run around 37 min. As for mass spectrometry (MS), the electron ionisation with 70 eV was used to detect the mass fragment at scan range between 50 and 550 m/z. The ion source temperature and transfer line have been set at 200 °C and 300 °C, respectively. The GC peak areas were integrated, and the component identification was done by comparing the MS with standards and with a library search (National Institute of Standard and Technology, NIST, USA).

2.6 Antimicrobial activity

Disk inhibitory assay was carried out using method described by Hudzicki [22]. Sterilised commercial disk (Whatman, England) with a diameter of 6.0 mm was added with 30 µL of CACE (100 mg/mL). Methanol and commercial disks impregnated with kanamycin (30 µg/mL) were used as negative and positive control, respectively. The sample impregnated disks were left air-dried in the biological safety cabinet (ESCO Class II BCC, Singapore). *Staphylococcus aureus* bacterial suspension was prepared by

inoculating 5–10 loops of single colony bacteria into 5 mL of sterile saline water (0.9% w/v sodium chloride solution). The turbidity of the bacterial suspension was compared and adjusted to 0.5 McFarland standard solution. Pre-sterilised cotton swab was used to inoculate the prepared bacterial suspension onto Mueller Hinton agar and left for 10 min. The prepared disks were aseptically transferred onto the surface of the agar plate and labelled. The agar plate was inverted and incubated at 37 °C for 24 h. The diameter of the inhibition zones formed around the disk directly indicates the extent of antibacterial activity for CACE. The experiment was carried out in triplicates. The experiment was repeated using *Pseudomonas aeruginosa* (*P. aeruginosa*), *Enterococcus faecalis* (*E. faecalis*) and *Escherichia coli* (*E. coli*). The antifungal activities of CACE were determined using methods as suggested by Kartal et al. [23]; three fungi strains (*Aspergillus niger*, *A. niger*; *Fusarium oxysporum*, *F. oxysporum*; and *Candida albicans*, *C. albicans*) were aseptically transferred using inoculating loop into a series of sterilised universal bottle (28 × 85 mm) containing 5 mL of autoclave-sterilised distilled water. Sufficient inoculum was adjusted until the turbidity equals to 0.5 McFarland standard solution. Then, 100 µL of each inoculum was incorporated in 20 mL of potato dextrose agar, PDA (M096-500G, HiMedia). The mixture was poured into 90-mm petri dishes and swirled left and right before left on the bench to solidify. Three mm diameter wells were punched into the agar by using sterilised cork borer. Then, 50 µL of CACE (2–10 mg/mL in methanol) were added into the wells followed by incubation at 37 °C for 24 h. The antifungal activities were evaluated by measuring the diameter of the halo-zone formation around the well. Similar experimental procedure was carried out using 3% copper chromium boron (CCB) sample acting as positive control and methanol as negative control.

2.7 Statistical analysis

All values were expressed as mean ± standard deviation (S.D) of triplicate measurements calculated using the Microsoft excel spreadsheet. The significant differences from the respective controls were tested using Pearson's t-test SPSS Statistics package for each set of experiment.

3 Results and discussion

3.1 Characterisation of PKS

PKS used has the following characteristics (in wt. %): ash content (0.68 ± 0.08), moisture (7.00 ± 0.08), volatile matter content (88.45 ± 2.38), fixed carbon content (3.87 ± 0.26), nitrogen (0.39 ± 0.02), carbon (51.60 ± 0.58), hydrogen (6.65 ± 0.08), sulphur (0.22 ± 0.08), oxygen (41.14 ± 0.57),

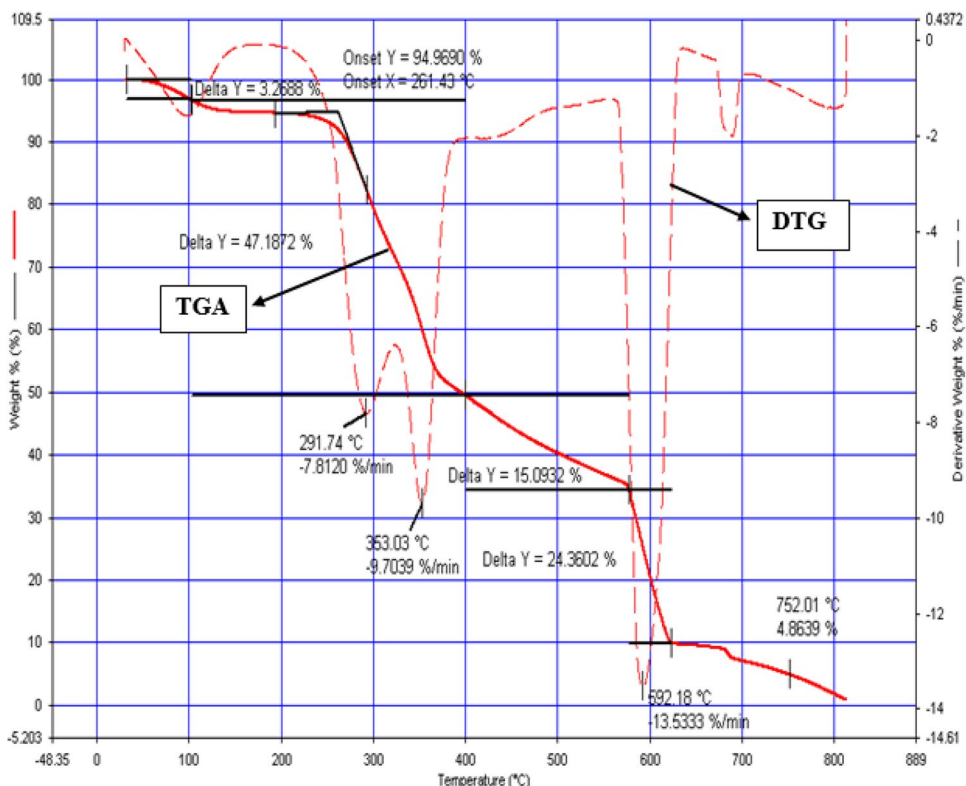
lignin (48.52 ± 0.63), acid soluble lignin (1.57 ± 0.08), acid insoluble lignin (46.95 ± 0.03), cellulose (33.61 ± 0.22), hemicellulose (17.87 ± 0.08) and extractives (4.26 ± 0.08). Lignin content analysis is an important measure to indicate the expected yield of phenolic compounds in AC such as pyrocatechol, phenol, syringol, guaiacol and its alkylated derivatives [24]. The lignocellulosic contents in PKS biomass also fall within the typical reported range for biomass, i.e. 20–40% for cellulose, 20–30% (hemicellulose) and 10–25% for lignin [25, 26].

From the TG-DTG analysis (30–850 °C) as shown in Fig. 1, three different regions were clearly distinguishable from the TG curve. The first region indicated initial weight loss of PKS (3.27 wt. %, <200°C) due to the removal of water content. The second region (weight loss around 47.19 wt. %, 250–380 °C) represented the decomposition of cellulose, hemicellulose and some part of lignin, respectively, into biochar [27] and was the region where major devolatilisation of PKS was observed (indicated from the steeper TG curve). In the third region (600–850 °C), around 24.36 wt. % of PKS were lost due to the slow decomposition of biochar to produce ash which can be substantiated from the presence of two small peaks at 700 °C and 800 °C [27]. For the DTG curve, the first two double peaks indicated a two-step thermal decomposition reaction mechanism that occurred at 291.74 °C (hemicellulose) and 363.03 °C (cellulose). The double peaks were indistinguishable to each other as the almost similar percentage of hemicellulose and cellulose content in PKS. The third peak observed at 592.18 °C can be attributed to devolatilisation and oxidation of char in PKS that produced 24.36 wt. % of ash. This is mainly due to the decomposition of the remaining lignin content at 500–900 °C [27]. This observation was similar to a report where the occurrence of hemicellulose decomposition was recorded at 220–315 °C, cellulose at 315–400 °C and lignin at 160–900 °C (due to its higher thermal stability) [28].

3.2 Pyrolysis products yields

The highest yield of AC, tar, biochar and biogas was recorded at 29.1 wt% (Std 16), 17.4 wt% (Std 4), 71.4 wt% (Std 9) and 51.4 wt% (Std 3), respectively (Fig. 2). Lower final temperature would favour the production of solid (char), while higher final temperature would favour liquid products (AC and bio-oil). The highest AC yield of 29.1 wt% (Std 16) was achieved at nitrogen flow rate of 3 L/min, microwave power of 575 W and final temperature of 450 °C. Similar operating condition resulted in comparable yield for AC and char (for standard 15th to 17th), but yield for tar and gas was different. There was significant increase in AC when the final temperature was increase from 198 to 450 °C. A further increase in temperature to 702 °C did not result in a significant decrease in AC yield (27.04 wt %) rather

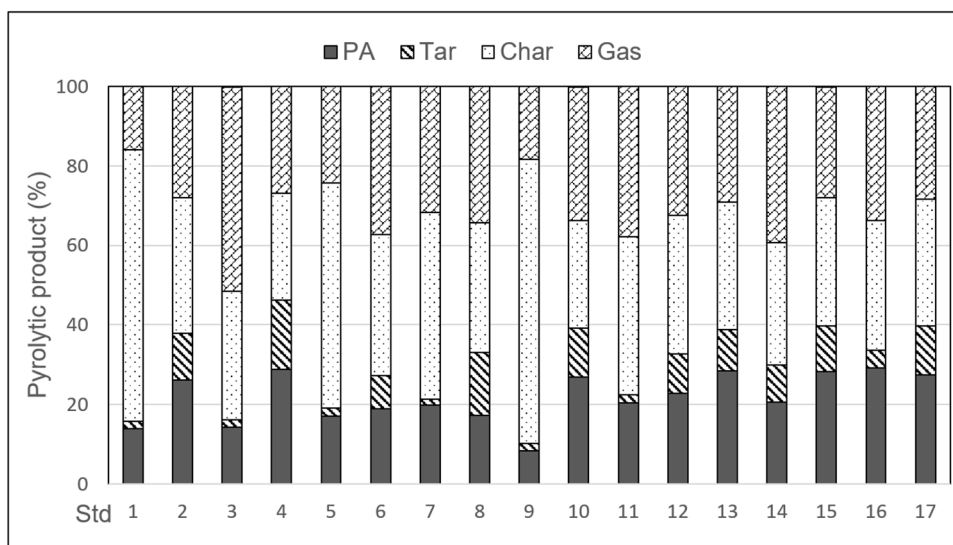
Fig. 1 TGA-DTG curve profile of PKS biomass



increase in the production of pyrolytic gas. The increase in pyrolytic gas be attributed to (1) fragmentation of primary mechanism that results in the formation of incondensable gas and (2) thermal cracking of secondary mechanism that

leads to smaller molecular weight molecules, where both favours condition with higher temperature than 600 °C [29]. These results were supported by other studies where biomass lignocellulosic material was volatile with a maximum liquid

Fig. 2 Pyrolysis product distribution of PKS under different final temperature (FT), microwave power (MP) and nitrogen flow rate (NFR) according to RSM method



FT (°C)	300	600	300	600	300	600	300	600	198	702	450						
MP (W)	350		800		350		800		575		350	800	575				
NFR (L/min)	1.0				5.0				3.0					1.0	6.4	3.0	

*Std = Standard, FT = Final temperature, MP = Microwave power, NFR = Nitrogen flow rate

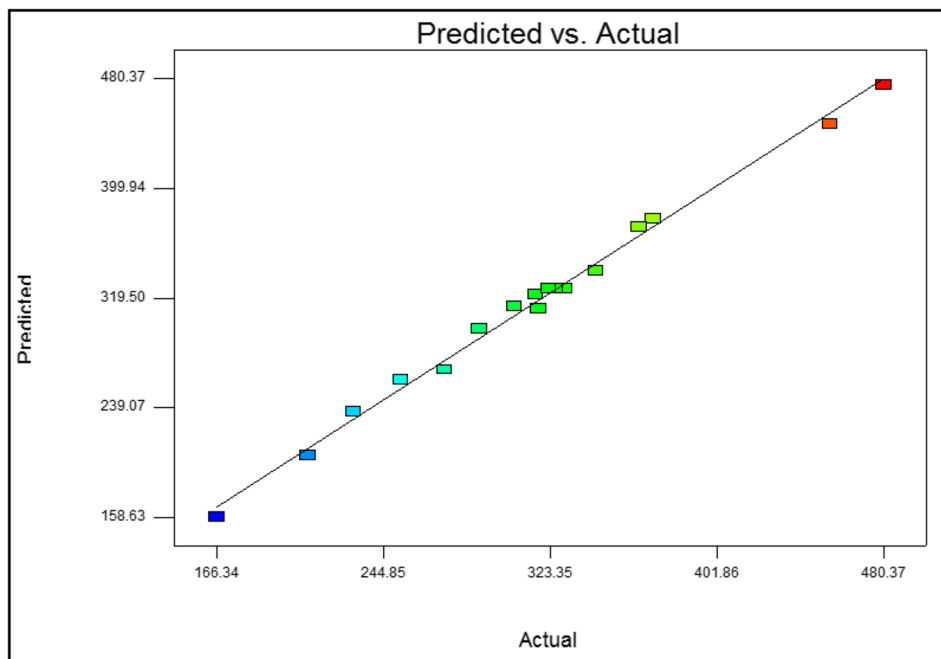
Table 2 Analysis of variance (ANOVA) for total phenolic content of AC

Source	Sum of squares	DF	Mean square	F value	Prob > F	Remark
Model	11,618.94	9	11,618.94	59.21	<0.0001	Significant
A	417.55	1	417.55	20.13	0.0488	Significant
B	11,284.90	1	11,284.90	57.51	0.0001	Significant
C	12,491.03	1	12,491.03	63.65	<0.0001	Significant
A ²	15,639.46	1	15,639.46	79.70	<0.0001	Significant
B ²	59,964.51	1	59,964.51	305.57	<0.0001	Significant
C ²	36,223.19	1	36,223.19	184.59	<0.0001	Significant
AB	4271.65	1	4271.65	21.77	0.0023	Significant
AC	98.70	1	98.70	0.50	0.5011	
BC	20.80	1	20.80	0.11	0.7543	
Residual	1373.67	7	196.24			
Lack-of-fit	330.28	5	66.06	0.13	0.9717	Not significant
Pure error	1043.39	2	521.70			
Cor total	11,618.95	16				
Model suggested						Quadratic
R ²						0.9870
Adj. R ²						0.9704
Pred. R ²						0.9543
Adeq. R ²						24.16

yield at temperature between 350 and 600 °C during pyrolysis process [18, 30, 31].

Microwave power is directly related to heating rate [32]. The application of microwave power at a higher level leads to higher heating rate and faster release of larger volatiles (both in liquid and gas forms). This situation was noticeable from this study where the char yield was reduced when the microwave power was increased from 350 to 800 W. The percentage yield of AC did not reveal any significant changes

when the microwave power was changed, thus highlighting the more significant effect of final temperature towards the distribution of pyrolysis products. For the effect of nitrogen flow, AC production was decreased from 28.43 wt% (Std 13) to 20.59 wt% (Std 14) as the nitrogen flow rate was increased from 1 to 6.4 L/min. This trend was also observed at 600 °C regardless of the variation in microwave power used (350 W and 600 W) as reduced AC yield was observed, i.e. 26.06 wt% to 18.85 wt% (for 350 W) and 28.76 wt% to 17.22 wt%

Fig. 3 Predicted versus actual of total phenolic content of AC

(for 600 W). Much less AC collected can be attributed to the shorter vapour residence time in the condenser tube that yielded more non-condensable gas [33].

3.3 Optimisation of TPC

The highest TPC concentration was 480.01 µg GAE/mg at microwave power of 575 W, final temperature of 450 °C and nitrogen flow rate of 3.0 L/min (Std 15), while the lowest TPC was 190.12 µg GAE/mg when the microwave power of 350 W, nitrogen flow rate of 1.0 L/min and final temperature of 600 °C (std 2), as shown in Table 1. This result clearly indicates the importance of high nitrogen flow rate and high microwave power to get higher TPC value. Phenolic constituents were derived from the decomposition of lignin in PKS. Similar finding was also reported where the maximum yield of TPC was obtained when the weight loss of lignin was maximum (at 450 °C) [34].

The correlation between the response TPC concentrations (Table 1) with the three factors was determined using multiple regression analysis and represented as polynomial equation as shown in Eq. (1), while results from the analysis of variance (ANOVA) are as summarised in Table 2. The quadratic model fitted the optimisation of TPC concentration with determination coefficient (R^2) of 0.9870 (with adjusted R^2 of 0.9543). The R^2 value indicates that 98.70% of the total variation in the TPC of AC was attributed to the experimental variables studied. Thus, only 1.30% of the TPC was not explained by the model. The adequate R^2 value of 24.16 represents the signal-to-noise ratio. This ratio is greater than 4 which indicates an adequate signal, and therefore, the model is significant for the process.

$$\text{TPC} = 456.77 - 5.53 A + 28.75 B + 30.24 C + 23.11 AB + 3.51 AC - 1.61 BC - 37.25 A^2 - 72.93 B^2 - 56.68 C^2 \quad (1)$$

As shown in Table 2, the provided model was significant for TPC concentration of AC as proved by the P-value of less than 0.0001 and F value of 59.21. The most significant parameter was nitrogen flow rate as F value was the highest as compared to the other two factors. In addition, final temperature (A), microwave power (B), nitrogen flow rate (C), A^2 , B^2 , C^2 and AB have a significant effect on the TPC concentration with P-value less than 0.05. The lack-of-fit P-value of 0.9717 implies that it was not significant relative to the pure error. According to the equations, the reduction of factors A, A^2 , B^2 and C^2 would increase the TPC, while increasing the other factors would increase the TPC concentration of AC.

The graph for predicted versus actual values of total phenolic content in AC, as depicted in Fig. 3, indicates the capability of the developed quadratic models to satisfactorily adjust to the experimental data, as well as limit the

percentage error between predicted and actual experimental results. The interaction between two factors was also evaluated as quadratic model was used. It can be observed that both the final temperature and microwave power play significant roles in the production of TPC at optimum condition (Fig. 4a). The production of TPC increased as the final temperature increased from 300 to 480 °C while became constant as temperature increased beyond 480 °C at constant microwave power of 575 W.

The validation test was carried out (in triplicates) based on the limited constraint range and the solution suggested by CCD in RSM of Design-Expert software. The criteria for all factors were in the ranges with the maximum goal for both responses. From the software, the optimised parameters suggested were as follows: final temperature of 480 °C, microwave power of 580 W and nitrogen flow rate of 2.4 L/min which would give a maximum predicted value of 461.10 µg GAE/mg sample of AC. After the validation tests were carried out, the maximum TPC concentration of 451.51 ± 2.37 mg µg GAE/mg sample of AC was obtained which was in good agreement with the predicted value with a standard deviation of 1.2%. The optimised TPC value was much higher compared to that reported for oil palm fibre (26.61 ± 0.96 mg gallic acid/g) [18] and pineapple waste biomass (9.50 ± 0.11) [3].

3.4 Antioxidant activity

Microwave-assisted AC showed high potency for DPPH radical scavenging with IC_{50} value of 39.83 ± 2.11 µg/mL µg/mL which is similar to ascorbic acid

(38.89 ± 1.55 µg/mL). This finding is supported by other researchers such as Ma et al. [35] who studied the antioxidant of AC from walnut shell and Ma et al. [5] who studied the AC obtained from *Rosmarinus officinalis* leaves. The IC_{50} for *R. officinalis* leaves ranged from 16 ± 0.2 to 31 ± 0.26 µg/mL, while Mathew and Zakaria [3] reported that the AC extract from pineapple waste biomass exhibited 89.7% of DPPH radical scavenging capacity at 25 µg/mL. The scavenging effects of CACE increased with the concentrations of the extracts. From the TEAC assay, CACE exhibited a higher TEAC value (1096.24 ± 3.56 µg TE/ mg) than ascorbic acid (951.26 ± 3.27 µg TE/mg. High TEAC values can be partly attributed to the TEAC level of 3-methoxycatechol, catechol and syringol of 1039 ± 51 , 1022 ± 53 and 956 ± 40 µg TE/ mg of the sample, respectively, as reported by Loo et al. [19].

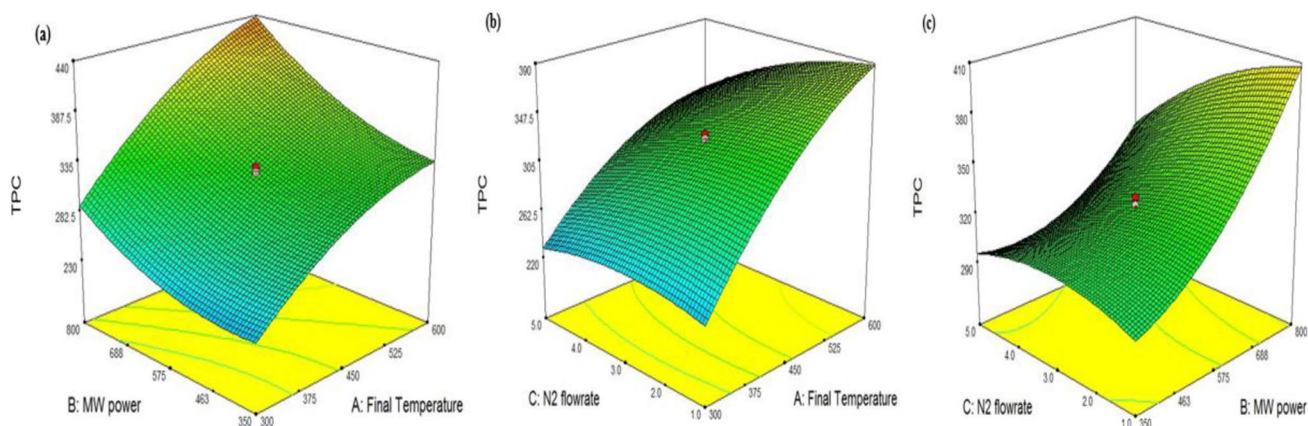


Fig. 4 3D surface graph of factors interaction towards TPC of PA against **a** final temperature and microwave power (AB), **b** final temperature and nitrogen flow rate (AC) and **c** microwave power and nitrogen flow rate (BC)

3.5 GC–MS analysis

From the GC–MS analysis, 20 chemical compounds were determined from CACE which phenols and its derivatives being the major compounds followed by organic acids, ketones, furan and pyran derivatives (Table 3). CACE consisted of phenolic derivatives (78.56%) with the major compounds being 1,2-benzenediol, i.e. catechol (27.82%), 1,3-dimethoxy-2-hydroxybenzene, i.e. syringol (22.76%) and 2-methoxyphenol, i.e. guaiacol (5.19%). A small percentage of organic acids (7.14%) were also present (acetic acid, 7.07%, and 4-hydroxybenzoic acid, 9.29%) as well as ketones (4.87%) and furan and pyran derivatives (1.76%). CACE from pineapple waste has been reported to have high content of phenolic compounds (69.5%) with the presence of 2,6-dimethoxy phenol, 1,2-benzenediol, 3-methoxy 1,2-benzenediol and 2-methoxy phenol [3]. Thermal degradation of lignin that takes place in temperature ranges from 160 to 600 °C leads to the production of high amount of phenol, guaiacol, syringol, creosol and other phenolic compounds as they were released due to cleavage of ether linkages among the lignin units [34, 36]. The presence of furan and pyran derivatives, ketones and organic acids was mainly derived from the decomposition of cellulose and hemicelluloses [29, 37].

3.6 Antimicrobial activity

The optimised CACE showed antimicrobial activities (based on the formation of inhibition zone) against all pathogenic bacteria in the following order: *S. aureus* (22.50 ± 0.86 mm) > *E. coli* > *P. aeruginosa* > *E. faecalis*. These results was supported from previous reports on antibacterial activity of AC extract from oil palm biomass [38, 39]. Ibrahim et al. also reported a broad-spectrum activity of AC from *Rhizophora apiculata* including *Bacillus*

subtilis, *B. cereus*, *B. spizizenii*, *S. aureus* and *S. epidermidis* [40]. This antimicrobial capability of CACE can be attributed to the presence of hydroxylated phenolic compounds [9]. Catechol and pyrogallol are known to have antimicrobial activity that increases with increasing hydroxyl group [41, 42]. Kanamycin exhibited broad-spectrum antibacterial activity as inhibition zone was observed against all tested pathogenic bacteria. Kanamycin was least effective against *P. aeruginosa* with zone of inhibition diameter of 24.33 ± 0.58 mm. Negative control did not exhibit inhibition zone as methanol was completely evaporated during the disk preparation (Table 4).

The results obtained from the resulting inhibition zone (in mm) suggested the effectiveness of antifungal activities for samples towards *C. albicans*, *A. niger* and *F. oxysporum* as follows: 3% CCB (positive control) > CACE > methanol (negative control). At a concentration of sample used (10 mg/ mL), 3% CCB showed inhibition zone values of 66 ± 3.65 mm (*A. niger*), 58 ± 2.17 mm (*F. oxysporum*) and 76 ± 2.54 mm (*C. albicans*), while lower values were obtained for CACE (52 ± 0.39 mm, *A. niger*; 48 ± 4.86 mm, *F. oxysporum*; and 58 ± 0.66 mm, *C. albicans*). Other sources of AC such as that of *Eucalyptus urograndis*, *Mimosa tenuiflora* and *Rhizophora apiculata* were reported to have good antifungal activity with 8–22-mm growth inhibition zone against *C. albicans* and *Cryptococcus neoformans* [7, 9]. High antifungal capacities for CACE can be attributed to its higher TPC content (480.01 µg GAE/mg) as antifungal properties of AC are strongly dependent on phenolic contents [43]. The result was also supported by the findings where the synergistic activity of various phenolics in PAs was responsible for good antifungal rather than the activity of any single phenol compound [23]. Fungal growth inhibition can be caused by the alteration of fungi cell wall, disruption of plasma membranes, inhibition on membrane plasma permeability (protein translocation,

Table 3 GC–MS analysis of CACE

No	Compounds	Molecular formula	Retention time (min)	Relative contents (%)
Phenols and derivatives				78.56
1	Phenol	C ₆ H ₆ O	4.020	2.24
2	2-Methylphenol	C ₇ H ₈ O	9.799	2.21
3	4-Methylphenol	C ₇ H ₈ O	10.400	2.29
4	2-Methoxyphenol	C ₇ H ₈ O ₂	10.731	5.19
5	3-Ethylphenol	C ₈ H ₁₀ O	13.066	0.42
6	2-Methoxy-4-methylphenol	C ₈ H ₁₀ O ₂	13.695	3.32
7	1,2-Benzenediol	C ₆ H ₆ O ₂	13.993	27.82
8	3-Methoxy-1,2-benzenediol	C ₇ H ₈ O ₃	15.595	2.13
9	4-Ethyl-2-methoxyphenol	C ₉ H ₁₂ O ₂	16.087	4.02
10	2,3-Dimethylphenol	C ₈ H ₁₀ O	12.471	0.24
11	2,6-Dimethoxy-4-(2-propenyl)-phenol	C ₁₁ H ₁₄ O ₃	16.004	5.92
12	1,3-Dimethoxy-2-hydroxybenzene	C ₈ H ₁₀ O ₃	8.15	22.76
Ketones				4.87
13	2-Cyclopenten-1-one	C ₅ H ₆ O	5.639	3.6
14	1-(2,4-Dihydroxyphenyl)ethanone	C ₈ H ₈ O ₃	0.86	0.86
15	3-Methyl-1,2-cyclopentanedione	C ₆ H ₈ O ₂	9.10	0.41
Organic acids				7.14
16	Acetic acid	C ₂ H ₄ O ₂	22.484	7.07
17	4-Hydroxybenzoic acid	C ₇ H ₆ O ₃	10.476	9.29
18	2,4-Hexadienedioic acid	C ₆ H ₆ O ₄	24.338	0.78
Furan and pyran derivatives				1.76
19	2,5-Dimethylfuran	C ₆ H ₈ O	7.207	1.48
20	3,4-Dihydro-2-methoxy-2H-pyran	C ₆ H ₁₀ O ₂	5.851	0.28

enzyme-dependent reaction) as well as inhibition of electron transport that resulted into ion leakage from the fungi cell [8]. The good antimicrobial activity of CACE indicated its potential applications in health-related and agricultural areas such as alternative treatment against microbial infection in human and colonisation of plant root systems by pathogenic microorganisms.

4 Conclusion

CACE derived from microwave-assisted pyrolysis of PKS exhibited promising antioxidant and antimicrobial activities. The optimisation of the microwave-assisted heating process is crucial to ensure that the highest yield of TPC can be obtained as shown in this study where the highest

Table 4 Zone of inhibition and relative inhibition percentages of CACE, kanamycin and CCB (positive control)

Bacterial strain	Zone of inhibition (mm)		Relative percentage of inhibition of CACE (%)
	CACE	Kanamycin/CCB	
<i>S. aureus</i> (ATCC 6538)	22.50 ± 0.86	35.25 ± 1.00	85.25 ± 3.82
<i>E. faecalis</i> (ATCC 29,212)	16.00 ± 1.00	31.33 ± 1.53	51.04 ± 0.90
<i>E. coli</i> (ATCC 11,229)	18.83 ± 1.04	30.33 ± 0.58	57.74 ± 3.91
<i>P. aeruginosa</i> (ATCC 15,442)	16.33 ± 0.57	24.33 ± 0.58	67.17 ± 3.44
Fungi strain			
<i>A. niger</i>	52 ± 0.39	66 ± 3.65	78.79 ± 4.69
<i>F. oxysporum</i>	48 ± 4.86	58 ± 2.17	82.76 ± 11.06
<i>C. albicans</i>	58 ± 0.66	76 ± 2.54	76.32 ± 3.32

TPC content of $451.51 \pm 2.37 \mu\text{g GAE/mg}$ of AC were obtained at optimised parameters of final temperature of 480°C , microwave power of 580 W and nitrogen flow rate of 2.4 L/min . Nevertheless, more studies need to be carried out prior to any commercialisation attempts for processes such as this.

Funding The authors acknowledged the Ministry of Higher Education, Malaysia, for Research University (QJ130000.2451.07G78) grant and the Graduate Research Assistantship to Mohd. Amir Asyraf Mohd. Hamzah. Our sincere gratitude also goes to the Malaysian Palm Oil Board for the GSAS Scholarship to Seri Elyanie Zulkifli.

Data availability Not applicable.

Code availability Not applicable.

Declarations

Ethics approval Not applicable.

Consent to participate All authors have given consent to participate.

Consent for publication All authors have provided consent for publication.

Conflict of interest The authors declare no competing interests.

References

1. Malaysian-German Chamber of Commerce and Industry (2017) Oil palm biomass & biogas in Malaysia, 2017 - potential for European SMEs. EUMalaysia Chamb Commer Ind (EUMCCI). https://businessmalaysia.eu/admin/js/fileman/Uploads/BiomassBiogas2018_Final_20180508.pdf. Accessed 14 June 2021
2. Ahmad R, Hamidin N, Ali UFM, Abidin CZA (2015) Characterization of bio-oil from palm kernel shell pyrolysis. *J Mech Eng Sci* 7:1134–1140. <https://doi.org/10.15282/jmes.7.2014.12.0110>
3. Mathew S, Zakaria ZA (2015) Pyrolygneous acid—the smoky acidic liquid from plant biomass. *Appl Microbiol Biotechnol* 99:611–622. <https://doi.org/10.1007/s00253-014-6242-1>
4. Abnisa F, Daud WMAW, Husin WNW, Sahu JN (2011) Utilization possibilities of palm shell as a source of biomass energy in Malaysia by producing bio-oil in pyrolysis process. *Biomass Bioenerg* 35:1863–1872. <https://doi.org/10.1016/J.BIOMBIOE.2011.01.033>
5. Ma C, Song K, Yu J, Yang L, Zhao C, Wang W, Zu G, Zu Y (2013) Pyrolysis process and antioxidant activity of pyrolygneous acid from *Rosmarinus officinalis* leaves. *J Anal Appl Pyrolysis* 104:38–47. <https://doi.org/10.1016/j.jaap.2013.09.011>
6. Clark M, Tilman D (2017) Comparative analysis of environmental impacts of agricultural production systems, agricultural input efficiency, and food choice. *Environ Res Lett* 12:064016. <https://doi.org/10.1088/1748-9326/aa6cd5>
7. Araujo E de S, Pimenta AS, Feijó FMC, Castro RVO, Fasciotti M, Monteiro TVC, de Lima KMG (2018) Antibacterial and anti-fungal activities of pyrolygneous acid from wood of *Eucalyptus urograndis* and *Mimosa tenuiflora*. *J Appl Microbiol* 124:85–96. <https://doi.org/10.1111/jam.13626>
8. Yahayu M, Mahmud KN, Mahamad MN, Ngadiran S, Lipeh S, Ujang S, Zakaria ZA (2017) Efficacy of pyrolygneous acid from pineapple waste biomass as wood preserving agent. *J Teknol* 79:1–8. <https://doi.org/10.11113/jt.v79.9987>
9. Ibrahim D, Kassim J, Sheh-Hong L, Rusli W (2013) Efficacy of pyrolygneous acid from *Rhizophora apiculata* on pathogenic *Candida albicans*. *J Appl Pharm Sci* 3:7–13. <https://doi.org/10.7324/JAPS.2013.3702>
10. Rabiou Z, Hamzah MAAM, Hasham R, Zakaria ZA (2020) Characterization and antiinflammatory properties of fractionated pyrolygneous acid from palm kernel shell. *Environ Sci Pollut Res* 1–9. <https://doi.org/10.1007/s11356-020-09209-x>
11. Aguirre JL, Baena J, Martín MT, Nozal L, González S, Manjón JL, Peinado M (2020) Composition, ageing and herbicidal properties of wood vinegar obtained through fast biomass pyrolysis. *Energies* 13:2418. <https://doi.org/10.3390/en13102418>
12. Suresh G, Pakdel H, Rouissi T, Brar SK, Diarra M, Roy C (2020) Evaluation of pyrolygneous acid as a therapeutic agent against *Salmonella* in a simulated gastrointestinal tract of poultry. *Braz J Microbiol* 51:1309–1316. <https://doi.org/10.1007/s42770-020-00294-1>
13. Kimura Y, Suto S, Tatsuka M (2002) Evaluation of carcinogenic/Co-carcinogenic activity of Chikusaku-eki, a bamboo charcoal by-product used as a folk remedy, in BALB/c 3T3 cells. *Biol Pharm Bull* 25:1026–1029. <https://doi.org/10.1248/bpb.25.1026>
14. Tiilikkala K, Fagernäs L, Tiilikkala J (2014) History and use of wood pyrolysis liquids as biocide and plant protection product. *Open Agric J* 4:111–118. <https://doi.org/10.2174/1874331501004010111>
15. Ferreira SLC, Bruns RE, da Silva EGP, dos Santos WNL, Quintella CM, David JM, de Andrade JB, Breikreitz MC, Jardim ICSF, Neto BB (2007) Statistical designs and response surface techniques for the optimization of chromatographic systems. *J Chromatogr A* 1158:2–14. <https://doi.org/10.1016/j.chroma.2007.03.051>
16. Zolgharnein J, Shahmoradi A, Ghasemi JB (2013) Comparative study of Box-Behnken, central composite, and Doehlert matrix for multivariate optimization of Pb (II) adsorption onto Robinia tree leaves. *J Chemom* 27:12–20. <https://doi.org/10.1002/cem.2487>
17. Mensah RA, Jiang L, Asante-Okyere S, Qiang X, Jin C (2020) Kinetic parameter estimation from thermogravimetry and microscale combustion calorimetry. *Int J Mech Mechatron Eng* 14:54–63
18. Abas FZ, Ani FN, Zakaria ZA (2018) Microwave-assisted production of optimized pyrolysis liquid oil from oil palm fiber. *J Clean Prod* 182:404–413. <https://doi.org/10.1016/j.jclepro.2018.02.052>
19. Loo AY, Jain K, Darah I (2008) Antioxidant activity of compounds isolated from the pyrolygneous acid, *Rhizophora apiculata*. *Food Chem* 107:1151–1160. <https://doi.org/10.1016/j.foodchem.2007.09.044>
20. Athmouni K, Belghith T, Bellassouad K, El Feki A, Ayadi H (2015) Effect of extraction solvents on the biomolecules and antioxidant properties of *Scorzonera undulata* (Asteraceae): application of factorial design optimization phenolic extraction. *Acta Sci Pol Technol Aliment* 14:313–320. <https://doi.org/10.17306/J.AFS.2015.4.32>
21. Re R, Pellegrini N, Proteggente A, Pannala A, Yang M, Rice-Evans C (1999) Antioxidant activity applying an improved ABTS radical cation decolorization assay. *Free Radic Biol Med* 26:1231–1237. [https://doi.org/10.1016/S0891-5849\(98\)00315-3](https://doi.org/10.1016/S0891-5849(98)00315-3)
22. Biemer JJ (1973) Antimicrobial susceptibility testing by the Kirby-Bauer disc diffusion method. *Ann Clin Lab Sci* 3(2):135–140
23. Kartal SN, Yoshimura T, Imamura Y (2009) Modification of wood with Si compounds to limit boron leaching from treated wood and to increase termite and decay resistance. *Int Biodeterior Biodegrad* 63:187–190. <https://doi.org/10.1016/j.ibiod.2008.08.006>

24. Wei Q, Ma X, Zhao Z, Zhang S, Liu S (2010) Antioxidant activities and chemical profiles of pyrolygneous acids from walnut shell. *J Anal Appl Pyrolysis* 88:149–154. <https://doi.org/10.1016/j.jaap.2010.03.008>
25. Yang H, Yan R, Chen H, Lee DH, Zheng C (2007) Characteristics of hemicellulose, cellulose and lignin pyrolysis. *Fuel* 86:1781–1788. <https://doi.org/10.1016/j.fuel.2006.12.013>
26. Stefanidis SD, Kalogiannis KG, Iliopoulou EF, Michailof CM, Pilavachi PA, Lappas AA (2014) A study of lignocellulosic biomass pyrolysis via the pyrolysis of cellulose, hemicellulose and lignin. *J Anal Appl Pyrolysis* 105:143–150. <https://doi.org/10.1016/j.jaap.2013.10.013>
27. Abdullah SS, Yusup S, Ahmad MM, Ramli A, Ismail L (2010) Thermogravimetry study on pyrolysis of various lignocellulosic biomass for potential hydrogen production. *World Acad Sci Eng Technol* 72:129–133. <https://doi.org/10.5281/zenodo.1078693>
28. Nordin NIAA, Ariffin H, Andou Y, Hassan MA, Shirai Y, Nishida H, Yunus WMZW, Karuppuchamy S, Ibrahim NA (2013) Modification of oil palm mesocarp fiber characteristics using superheated steam treatment. *Molecules* 18:9132–9146. <https://doi.org/10.3390/molecules18089132>
29. Collard FX, Blin J (2014) A review on pyrolysis of biomass constituents: mechanisms and composition of the products obtained from the conversion of cellulose, hemicelluloses and lignin. *Renew Sustain Energy Rev* 38:594–608. <https://doi.org/10.1016/j.rser.2014.06.013>
30. Abhijeet P, Swagathnath G, Rangabhashiyam S, Asok Rajkumar M, Balasubramanian P (2020) Prediction of pyrolytic product composition and yield for various grass biomass feedstocks. *Biomass Convers Biorefinery* 10:663–674. <https://doi.org/10.1007/s13399-019-00475-5>
31. Westerhof RJM, Brilman DWF, Van Swaaij WPM, Kersten SRA (2010) Effect of temperature in fluidized bed fast pyrolysis of biomass: oil quality assessment in test units. *Ind Eng Chem Res* 49(3):1160–1168. <https://doi.org/10.1021/ie900885c>
32. Wallace CA, Afzal MT, Saha GC (2019) Effect of feedstock and microwave pyrolysis temperature on physico-chemical and nano-scale mechanical properties of biochar. *Bioresour Bioprocess* 6:33. <https://doi.org/10.1186/s40643-019-0268-2>
33. Pütün E (2010) Catalytic pyrolysis of biomass: effects of pyrolysis temperature, sweeping gas flow rate and MgO catalyst. *Energy* 35:2761–2766. <https://doi.org/10.1016/j.energy.2010.02.024>
34. Wu Q, Zhang S, Hou B, Zheng H, Deng W, Liu D, Tang W (2015) Study on the preparation of wood vinegar from biomass residues by carbonization process. *Bioresour Technol* 179:98–103. <https://doi.org/10.1016/j.biortech.2014.12.026>
35. Ma X, Wei Q, Zhang S, Shi L, Zhao Z (2011) Isolation and bioactivities of organic acids and phenols from walnut shell pyrolygneous acid. *J Anal Appl Pyrolysis* 91:338–343. <https://doi.org/10.1016/j.jaap.2011.03.009>
36. Ma C, Li W, Zu Y, Yang L, Li J (2014) Antioxidant properties of pyrolygneous acid obtained by thermochemical conversion of *Schisandra chinensis* baill. *Molecules* 19:20821–20838. <https://doi.org/10.3390/molecules191220821>
37. Fernandez Y, Arenillas A, Angel J (2011) Microwave heating applied to pyrolysis. *Adv Induction Microw Heat Miner Org Mater*. <https://doi.org/10.5772/13548>
38. Mahmud KN, Yahayu M, Sarip SHM, Rizan NH, Min CB, Mustafa NF, Ngadiran S, Ujang S, Zakaria ZA (2016) Evaluation on efficiency of pyrolygneous acid from palm kernel shell as antifungal and solid pineapple biomass as antibacterial and plant growth promoter. *Sains Malaysiana* 45:1423–1434
39. Abas FZ, Zakaria ZA, Ani FN (2018) Antimicrobial properties of optimized microwave-assisted pyrolygneous acid from oil palm fiber. *J Appl Pharm Sci* 8:65–71. <https://doi.org/10.7324/JAPS.2018.8711>
40. Ibrahim D, Kassim J, Lim S, Rusli W, Biotechnology I (2014) Evaluation of antibacterial effects of *Rhizophora apiculata* pyrolygneous acid on pathogenic bacteria. *Malays J Microbiol Pathog Bact* 10:197–204
41. Cowan MM (1999) Plant products as antimicrobial agents. *Clin Microbiol Rev* 12:564–582. <https://doi.org/10.1128/cmr.12.4.564>
42. Kocaçalışkan I, Talan I, Terzi I (2006) Antimicrobial activity of catechol and pyrogallol as allelochemicals. *Zeitschrift fur Naturforsch - Sect C J Biosci* 61:639–642. <https://doi.org/10.1515/znc-2006-9-1004>
43. Baimark Y, Niamsa N (2009) Study on wood vinegars for use as coagulating and antifungal agents on the production of natural rubber sheets. *Biomass Bioenergy* 33:994–998. <https://doi.org/10.1016/j.biombioe.2009.04.001>

Publisher's note Springer Nature remains neutral with regard to jurisdictional claims in published maps and institutional affiliations.